INTERNATIONAL JOURNAL OF GEOMETRY
Vol.3 (2014), No. 2, 35 - 50

CONSTANT CURVATURE HYPERSURFACES IN $\mathcal{G}^m$

CASEY DOUGLAS

Abstract. In this article we discuss the basic geometry of curves in the Gauss plane with constant weighted-curvature. These curves help us understand hypersurfaces in Gauss space with constant weighted mean curvature. In particular, we characterize all embedded periodic and helicoidal minimal surfaces in Gauss space.

1. Introduction

As discussed in [14] and the references therein, Manifolds with Density are natural generalizations of Riemannian manifolds. They are obtained by equipping such a manifold, M, with a positive density $\Psi : M \to \mathbb{R}$ that is used to *equally* weight volume and hypsersurface area:

$$dV_\Psi = \Psi dV$$
$$dA_\Psi = \Psi dA$$

where dV and dA denote the Riemmanian volume and hyper surface area elements on M.

A particularly important example of a Manifold with Density is obtained by equipping Euclidean space $\mathbb{R}^m$ with the Gaussian probability density function

$$\Psi(\vec{x}) = (2\pi)^{-m/2}\exp\left(-\frac{1}{2}\|\vec{x}\|^2\right).$$

This space is known as Gauss Space, $\mathcal{G}^m$, and we will work with an equivalent version that is given by the rescaled density

$$\Psi(\vec{x}) = e^{\varphi(\vec{x})} \tag{1}$$

where $\varphi(\vec{x}) = -r^2/2$ and $r = \|\vec{x}\|$ denotes distance to the origin.

Keywords and phrases: Manifolds with Density, Gauss Space, Constant Curvature.
MSC 2010: Primary 53A04, Secondary 53A10.
Received: 10.07.2014. In revised form: 16.08.2014. Accepted: 10.09.2014

We continue to use the notation $\mathcal{G}^m$ in this setting and note that the quantity

$$H_\varphi = H - \frac{1}{m-1}\frac{d\varphi}{dn} \tag{2}$$

serves as a natural generalization of mean curvature for any function $\varphi(\vec{x})$ in (1) (see [11]). Expression (2) is sometimes referred to as weighted or φ-weighted mean curvature.

Of particular interest, then, are those hypersurfaces in $\mathcal{G}^m$ for which $H_\varphi = c$. Such hypersurfaces arise as potential solutions to weighted isoperimetric problems, for example. Curves in the Gauss Plane with constant weighted curvature have been studied in [2], as have weighted-geodesics (curves whose weighted curvature vanishes) in [7] and [4]. In Section 2 we discuss these curves and re-obtain many known results, but we do so via more accessible and inviting methods. As a result, we are able to expand upon known results and relate these curves to "self-shrinkers," curves that were studied and classified by Abresch and Langer in [1]. In Section 3 we classify all periodic and helicoidal minimal surfaces in $\mathcal{G}^m$.

2. Constant Weighted Curvature Hypersurfaces in $\mathcal{G}^2$

The Gaussian-weighted curvature of a curve $\gamma \subset \mathcal{G}^2$ is, according to (2), given by

$$k_\varphi = k - \frac{d\varphi}{dn} = k + h. \tag{3}$$

Here h is the *support function* of our curve $\gamma(t)$, itself given by

$$h = \langle \vec{x}, n \rangle$$

with $\vec{x}$ and n denoting the position and unit normal vectors, respectively. The support function for a hypersurface in $\mathbb{R}^m$ records the (oriented) distance from its tangent space to the origin.

When a locally convex curve is parameterized by its unit normal so that $n(t) = \pm e^{it}$, a straightforward calculation shows that

$$k(t) = -\frac{1}{h''(t) + h(t)}. \tag{4}$$

Under this parameterization, a curve with constant $k_\varphi = c$ will have a support function $h(t)$ that satisfies the equation

$$h''(t) = \frac{1}{h(t) - c} - h(t) \tag{5}$$

Moreover, a solution to (5) determines $\gamma(t)$ explicitly via the following equations.

$$\begin{aligned} x(t) &= h(t)\cos(t) - h'(t)\sin(t) \\ y(t) &= h(t)\sin(t) + h'(t)\cos(t) \end{aligned} \tag{6}$$

$$\gamma(t) = e^{it}(h(t) + ih'(t)) \tag{7}$$

Of course, if the (unweigthed) curvature vanishes, then parameterization by

the unit normal is not possible. Fortunately, it is easy to prove that every curve satisfying

$$k_\varphi = k + h = c \tag{8}$$

is, in fact, convex. This is contained in the following

Lemma 2.1. *If the support and curvature functions of a planar curve satisfy*

$$h \pm k = c$$

then either k is identically zero or never *vanishes. In other words, solutions are either lines or are convex.*

Proof. Suppose that γ is a solution curve whose curvature, k, vanishes at point (x_0, y_0). The tangent line through this point also solves (8) since $k = 0$ and $h = c$ at (x_0, y_0). By parameterizing γ as a graph, for instance, equation (8) is easily seen to meet the requirements for the Picard-Lindelof theorem ensuring existence and uniqueness of solutions. As a consequence, γ actually coincides with its tangent line, implying that $k \equiv 0$. □

Solutions to (5) give rise to constant Gaussian-weighted curvature curves via (6), and they share many properties with Gaussian-weighted geodesics. Our main result is Theorem 2.3, though, which states that for arbitrarily large values of c, there are many embedded curves with constant Gaussian-weighted curvature. This sits in stark contrast to the $c = 0$ case, where the only embedded curves are circles.

Constant solutions to (5) are given by $h = c_i$ where $1 = (c_i - c)\, c_i$ and $i \in \{1, 2\}$. One readily verifies

$$c = c_1 - \frac{1}{c_1} = c_2 - \frac{1}{c_2} \tag{9}$$

$$c_1 = \frac{c + \sqrt{c^2 + 4}}{2} \tag{10}$$

$$c_2 = \frac{c - \sqrt{c^2 + 4}}{2} \tag{11}$$

We also have $c_2 \leq c \leq c_1$, with equality if and only if $c = 0$ and $c_1 = 1 = -c_2$. These constant solutions produce circles of radius $|c_i|$ centered at the origin, and since no other closed form solutions are available, we impose initial conditions

$$h(0) = a \neq c \text{ and } h'(0) = \alpha. \tag{12}$$

Without loss of generality we set $h'(0) = \alpha = 0$, an assumption that is justified by integrating (5); indeed, this equation has the form

$$h'' = G'(h) \text{ where } G(h) = \ln(|h - c|) - h^2/2.$$

After adjusting constants, we obtain

$$\left(h'\right)^2 = \ln\left((h - c)^2\right) - h^2 + K. \tag{13}$$

As depicted in Figure 1, different values of K result in shifted plots of the function $F(h) = \ln\left((h - c)^2\right) - h^2$.

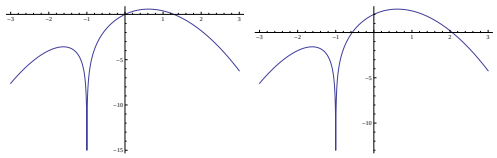

(A) $K = -F(c_1)$ (B) $K = 2$

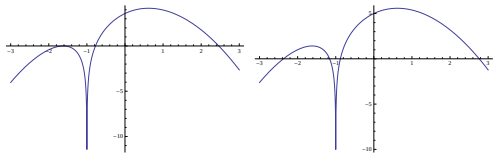

(C) $K = -F(c_2)$ (D) $K = 5$

FIGURE 1. Plots of $F(h)$ for $c = -1$

Constant solutions occur when $K = \min\{-F(c_i)\}$, and all larger choices of K imply the existence of points where $h' = 0$. Hence, we are free to set $h'(0) = \alpha = 0$. We can therefore rewrite (13) as

$$\left(h'\right)^2 = \ln\left((h-c)^2\right) - h^2 + a^2 - \ln\left((a-c)^2\right) = F(h) - F(a). \tag{14}$$

Note that for sufficiently large a, solutions to (5) come in pairs. Figure (1c) depicts a pairing between a constant solution and a non-constant one. The curves these paired-solutions give rise to do not coincide, except in the special case when $c = 0$.

Equation (14) allows us to sketch the phase plane for (h, h'), which, as indicated in Figure 2, is foliated by closed curves (and one vertical line corresponding to our singular solution). From this we deduce that solutions to (14) are periodic, a conclusion one can also argue via symmetry.

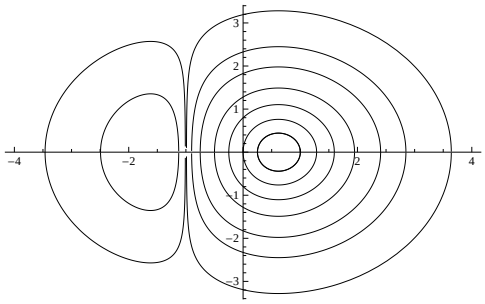

FIGURE 2. Phase Plot with $c = -1$

Let $P(a, c)$ denote the period of a solution to (5) with initial data $h(0) = a$ and $h'(0) = 0$. The half-period can be computed according to the formula

$$\frac{P}{2} = \int_{|b|}^{|a|} \frac{dx}{\sqrt{\ln\left((x-c)^2\right) - x^2 + a^2 - \ln\left((a-c)^2\right)}}. \tag{15}$$

The parameter a is chosen from the intervals $a \in (-\infty, c_2] \cup [c_1, \infty)$. This means that $b = h(P/2) \in [c_2, c) \cup (c, c_1]$ is determined by the relation

$$a^2 - \ln\left((a-c)^2\right) = b^2 - \ln\left((b-c)^2\right) \tag{16}$$

and so can be treated as an implicit function, $b = b(a, c)$. In particular, $a \in (-\infty, c_2] \iff b \in [c_2, c)$ and $a \in [c_1, \infty) \iff b \in (c, c_1]$ with $a \to \pm\infty \iff b \to c$.

When $a = c_i$, the support function $h = c_i$ is constant and γ is a circle. According to equation (6), non-circular curves will be closed if and only if $P \in 2\pi\,\mathbb{Q}$, a rather difficult condition to verify. Fortunately, we can establish the limiting behavior of the period with relative ease.

Theorem 2.1. *Suppose $h(t)$ satisfies (5) with $h(0) = a$ and $h'(0) = 0$. Then*

$$\lim_{a \to c_1^+} P(a, c) = \frac{2\pi}{\sqrt{1 + c_1^2}} \tag{17}$$

$$\lim_{a \to c_2^-} P(a, c) = \frac{2\pi}{\sqrt{1 + c_2^2}} \tag{18}$$

$$\lim_{a \to \pm\infty} P(a, c) = \pi \tag{19}$$

Proof. To establish (17) and (18) we first linearize (5) at its constant solutions c_i:

$$h'' = -(1 + c_i^2)h.$$

This is explicitly solved by

$$h(t) = A\cos\left(t\sqrt{1 + c_i^2}\right) + B\sin\left(t\sqrt{1 + c_i^2}\right).$$

Solutions with initial values a close to c_i will therefore have periods close to $2\pi(1 + c_i^2)^{-1/2}$, giving the desired limits.

Limit (19) is obtained by working explicitly with our period formula (15). One first sets $x = |a| \cdot u$, and this yields

$$\frac{P}{2} = \int_{|b/a|}^1 \frac{du}{\sqrt{1 - u^2 - G(a, u)}}.$$

The term $G(a, u)$ is given by

$$G(a, u) = \frac{\ln\left((a-c)^2\right) - \ln\left((au - c)^2\right)}{a^2}.$$

Making careful use of the facts that $\lim_{a \to \pm\infty} G(a, u) = 0$ (for any fixed u) and that $\lim_{a \to \pm\infty} b/a = 0$, we obtain the desired limit

$$\lim_{a \to \pm\infty} \frac{P}{2} = \int_0^1 \frac{du}{\sqrt{1 - u^2}} = \frac{\pi}{2}.$$

Alternatively, one can use the substitution $h(t) = aw(t)$ and solve

$$w'' = \frac{1}{a^2}\frac{1}{w} - w$$

$$w(0) = 1, \quad w'(0) = 0.$$

The limiting solution is given by $w = |\cos t|$. □

2.1. **The Geometry of Solution Curves.** Curves with constant Gaussian-weighted curvature exhibit a number of interesting geometric properties. For instance, all of them wind around or through the origin, "bouncing" between the boundaries of the annulus

$$\mathcal{A} = \{z \in \mathbb{C} \mid |b| \leq |z| \leq |a|\}.$$

We refer to the sets $\mathcal{A}$ as *enclosing annuli*, and they include certain degenerate annuli such as disks (when $b = 0$), circles (when $|a| = |b| = c_i$), and unbounded regions (when $|a| = \infty$ and $b = c$).

The support function $h(t)$ does not change sign if and only if b and a have the same sign. As seen in Fig 3,a non-vanishing support function results in a curve γ that will not cross itself before winding around (or passing through) the origin.

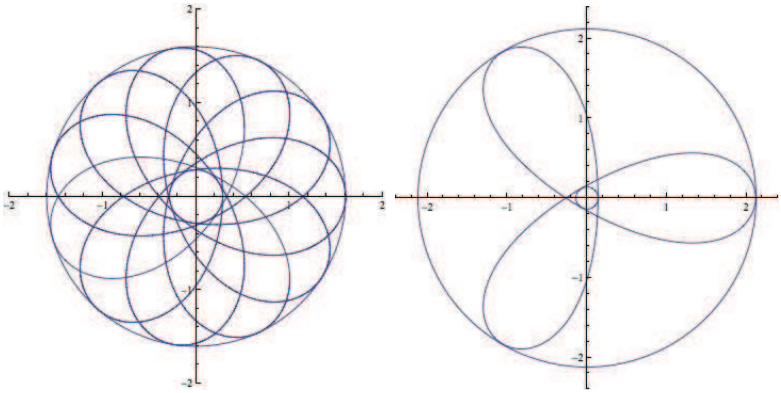

(A) $c = -0.25, a \approx 1.6, b \approx 0.29$ (B) $c = -0.1, a \approx 2.12, b \approx 0.139$

FIGURE 3. Strictly Positive Support Functions

However, if b and a have opposite signs, then self intersections occur before the curve has wound about the origin. This behavior is illustrated in Fig 4.

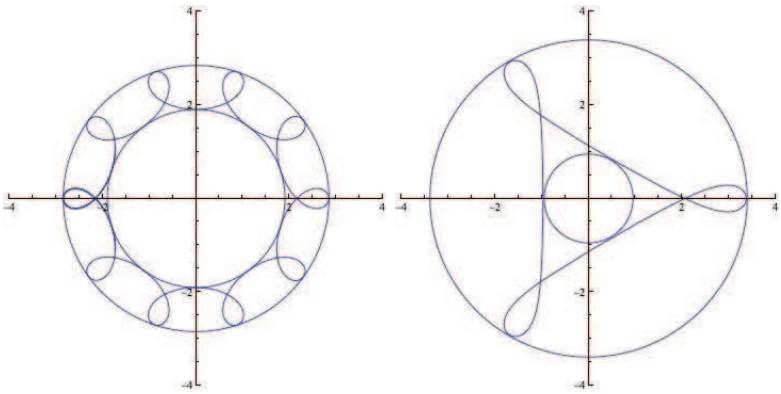

(A) $c = -0.25, a \approx 2.8, b \approx -1.9$ (B) $c = -1, a \approx 3.37, b \approx -0.95$

FIGURE 4. Support Function that changes sign

Both Figures 3 and 4 feature *closed* curves, ones with judiciously chosen a-values that ensure $P \in 2\pi\mathbb{Q}$. Of course, *most* of these curves do not behave so nicely. In general, they wind through a dense subset of $\mathcal{A}$ as indicated in Figure 5.

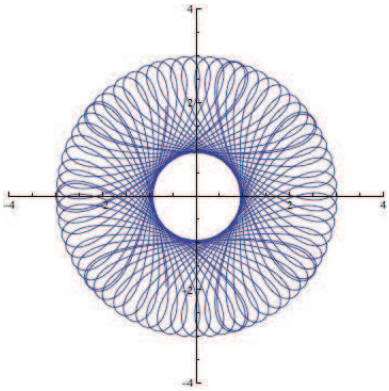

FIGURE 5. Annulus Filling Curve with $c = -1, a = 3, b \approx -.94$

Our observations about these curves follow easily from the explicit parameterization (6). For instance, one readily verifies that

$$r^2 = h^2 + (h')^2 = \ln((h-c)^2) + a^2 - \ln((a-c)^2)$$

and so $|b| \leq r \leq |a|$. Moreover, if we let $\theta(t)$ denote the angle between the positive x-axis and the position vector $\gamma(t) = (x(t), y(t))$, then a straightforward computation shows

$$\frac{d\theta}{dt} = \left(\frac{h}{h-c}\right)\frac{1}{r^2}$$

which implies that $dr/d\theta = 0$ when $r = |b|$ and $r = |a|$.

This agrees with the observation that at points where $\gamma(t) \in \partial\mathcal{A}$, the support function, h, attains its extreme values and, hence, so does the curvature k. At these points γ is said to have a *vertex*. It is also worth noting

that the infinitesimal arc-length of $\gamma(t)$ is given by

$$ds = \frac{dt}{|h-c|}.$$

One of the more pressing questions concerning our curves involves their period functions, $P(a,c)$, and the possibility of embeddedness.

Theorem 2.2. *The period P is bounded above by 2π.*

Proof. Suppose that for a given c there exists a such that $P/2 = \pi$. By construction, the curvature k is given by $k = h - c$ which will have extrema when $t \in (P/2)\,\mathbb{Z} = \pi\,\mathbb{Z}$. The curve γ, then, will be a simple closed curve with only two vertices. One is located at the point $(a, 0)$ and the other is located at $(-b, 0)$, but this contradicts the Four Vertex Theorem (consult [8] for an excellent treatment). Since $\lim_{a \to c_i} P(a) < 2\pi$ and since $P(a)$ is continuous in a, we therefore conclude that $P(a)$ remains bounded above by 2π. □

Theorem 2.3. *For $|c| > 14/\sqrt{15}$, there exist two or more embedded curves with constant Gaussian-weighted curvature c.*

Proof. We have already noted that in order for γ to be closed, the period $P(a,c)$ must be of the form $P(a,c) = 2\pi\, m/n$ where $m, n \in \mathbb{Z}$. This fraction encodes geometric information about γ. In particular, m is the winding number with respect to the origin, and n is the number of petals.

To see this we note that since the function $h(t)$ has reflectional symmetry at the points where $h' = 0$, so too does the solution curve γ. In particular, at these points (x_0, y_0), the curve γ may be reflected about the ray joining (x_0, y_0) to the origin. It follows that, for a closed solution curve, γ winds about the origin a total of m times.

Similarly, since the petals of γ occur where h (or, equivalently, k) has a maximum, there are necessarily n of them.

When a period is of the form $P(a,c) = 2\pi/n$ the resulting solution curve, γ, has n-fold symmetry and is necessarily embedded. The limits in Theorem (2.1) combined with equations (10) and (11) give us sufficient (but not necessary) conditions to conclude that $P(a,c)$ will have this form.

Specifically, we have that

$$\begin{matrix} P(c_1, c) \to 2\pi \\ P(c_2, c) \to 0 \end{matrix} \quad \text{as } c \to -\infty$$

$$\begin{matrix} P(c_1, c) \to 0 \\ P(c_2, c) \to 2\pi \end{matrix} \quad \text{as } c \to \infty$$

Hence, the limiting period, $P(c_i, c)$, can be made as small as we like, yielding any number of embedded solution curves. Moreover, by choosing a arbitrarily close to c_i, we obtain embedded solutions with as much reflectional symmetry as we like.

In particular, we find that $P(c_2) = \pi/2 \iff c_2 = -\sqrt{15} \iff c = -14/\sqrt{15}$. Similarly, $P(c_1) = \pi/2 \iff c_1 = \sqrt{15} \iff c = 14/\sqrt{15}$. It follows that if $|c| > 14/\sqrt{15}$ then, in addition to the circle corresponding to

$a = c_i$, there exists another embedded solution, and it has 4-fold symmetry. □

Figure 6 shows a graph of the period function $P(a, 6)$, which, as predicted by Theorem 2.3, attains the values $2\pi/6, 2\pi/5, 2\pi/4$, and $2\pi/3$. The embedded curves corresponding to the first three of these periods are shown below in Figures 6b, 6c, and 6d.

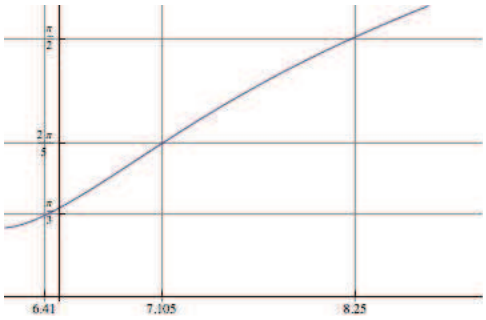

(A) $P(a, 6)$

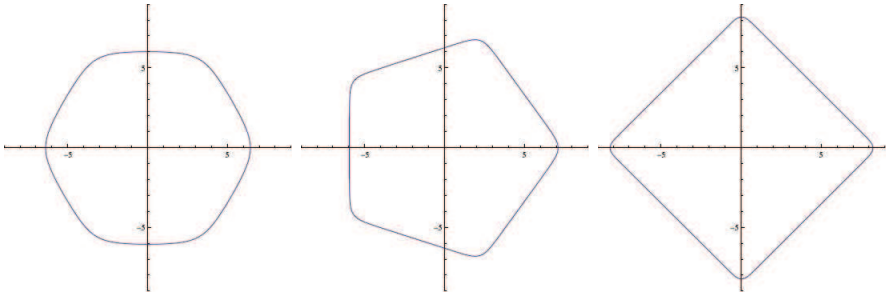

(B) $c = 6, a \approx 6.42$ (C) $c = 6, a \approx 7.105$ (D) $c = 6, a \approx 8.22$

FIGURE 6. Period Function $P(a, 6)$ and Embedded Curves

In general, the period functions $P(a, c)$ exhibit different behavior depending on c. When $c = 0$, the function is monotone decreasing for $a \geq 1$; moreover, for c *near* 0, $P(a, c)$ appears to be monotone decreasing on $[c_1, \infty)$ and monotone increasing on $(-\infty, c_2]$. However, as can be seen in Figure 7a, for sufficiently large large values of $|c|$, monotonicity can fail. More research is needed to better or fully understand the quantities

$$c^* = \sup\{c \geq 0 \mid P(a, c) \text{ is monotone on } [c_1, \infty)\}$$
$$c_* = \inf\{c \leq 0 \mid P(a, c) \text{ is monotone on } [c_1, \infty)\}$$

and the geometry of the curves to which they are associated.

Remark 2.1. *As noted in the proof of Theorem 2.3, the condition that* $|c| > 14/\sqrt{15}$ *is sufficient but* not *necessary. The values* $\pm 14/\sqrt{15}$ *are* not *sharp. Figure 7 shows period functions and embedded curves for values of* c *where* $|c| \leq 14/\sqrt{15}$.

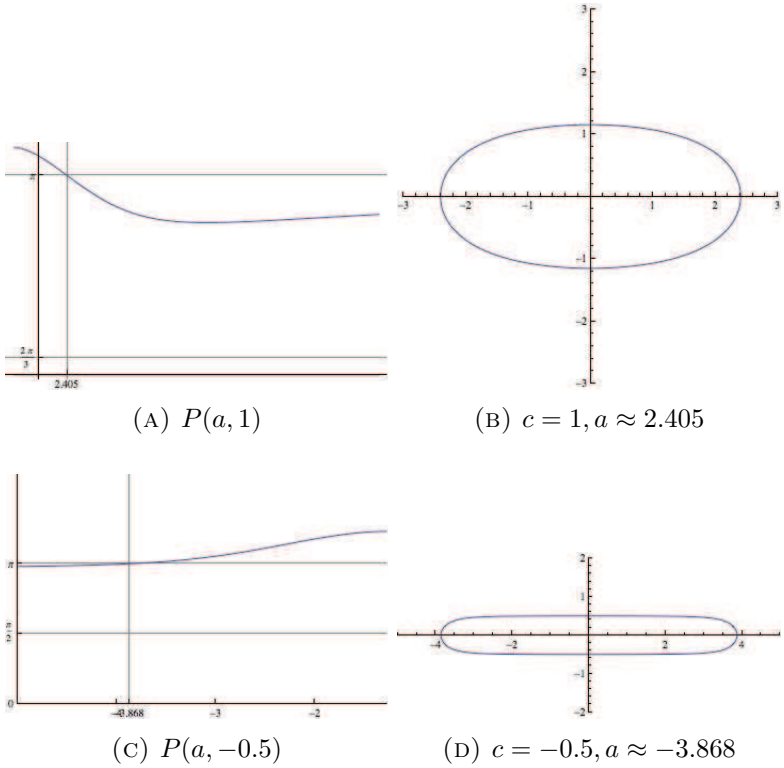

(A) $P(a, 1)$ (B) $c = 1, a \approx 2.405$

(C) $P(a, -0.5)$ (D) $c = -0.5, a \approx -3.868$

FIGURE 7. Period Functions (left) and embedded curves (right)

2.2. **Geodesics in $\mathcal{G}^2$ (The case when $c = 0$).** When $c = 0$ more can be said. These curves have support functions that *never* change sign, for instance, and they enjoy a so-called "areal paramaterization." This means that the amount of area swept out at $t = u$ depends linearly on u or, equivalently, that the parameterized curve's "areal velocity" and "angular momentum" are constant. Kepler's Second Law stipulates that the elliptical orbits of the planets enjoy this property, and, provided that $h \neq 0$, *any* curve can be furnished with such a parameterization. That our shrinkers have this property follows easily since

$$A(u) = \frac{1}{2}\int_0^u h(t)\, ds = \frac{1}{2}\int_0^u h(t)\frac{dt}{h(t)} = \frac{1}{2}\int_0^u dt = \frac{u}{2}.$$

We also note that in the $c = 0$ cases the enclosing annuli all enjoy a rather curious property. Their radii, a and b, are related via equation (16)

$$a^2 - \ln(a^2) = b^2 - \ln(b^2)$$

and this can be rearranged to produce the geometrically significant equation

$$\pi(a^2 - b^2) = 2\pi \ln\left(\frac{a}{b}\right).$$

The left-hand side is the Euclidean area of the enclosing annulus, $\mathcal{A}$, while the right-hand side is its "cylindrical area." In other words

$$\iint_{\mathcal{A}} dA = \iint_{\mathcal{A}} \frac{1}{r^2}\, dA$$

a notable equality since both metrics, $|dz|$ and $|z|^{-1}|dz|$, are conformally flat *and* solve classical extremal length problems (see [3]). That these weighted geodesics privilege such annuli suggests a deeper connection to complex analysis and conformal geometry.

When $c = 0$ we have $c_2 = -1$ and $c_1 = 1$, though, the function $(h')^2 = F(h)$ is symmetric about the y-axis.

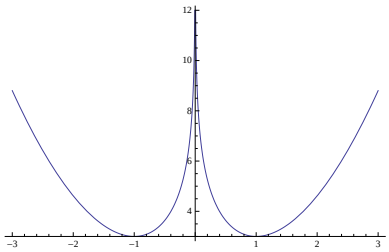

FIGURE 8. Plot of $F(h)$ for $c = 0$

As a consequence of this symmetry, we can take $a \in (1, \infty)$ so that $b \in (0, 1)$ with $a = b = 1$ if and only if γ parameterizes the unit circle. Moreover, we can further restrict the period, $P(a, 0) = P(a)$, of our curves' support functions.

Theorem 2.4. *The period function for a* strictly convex *Gaussian-weighted geodesic is bounded below by* π.

Proof. For a contradiction suppose $P(a) = \pi$ for some $a \in (1, \infty)$. Vertices for the resulting curve, γ, will occur at the points $(a, 0)$ and $(0, b)$ with curvature values $k = a$ and $k = b$, respectively. Our strategy, then, is to compare γ with the ellipse E:

$$\frac{x^2}{a^2} + \frac{y^2}{b^2} = 1.$$

This ellipse, E, and γ coincide at the points $(a, 0)$ and $(0, b)$, where both curves also share a tangent line. At the point $(a, 0)$, though, the curvature of our ellipse is greater than that of γ since $b \in (0, 1) \Rightarrow a/b^2 > a$. Conversely, at the point $(0, b)$, the curvature of our ellipse is less than that of γ since $b/a^2 < b$. These curvature conditions trap γ in the interior of the ellipse near $(0, b)$ but force it to the exterior near $(a, 0)$.

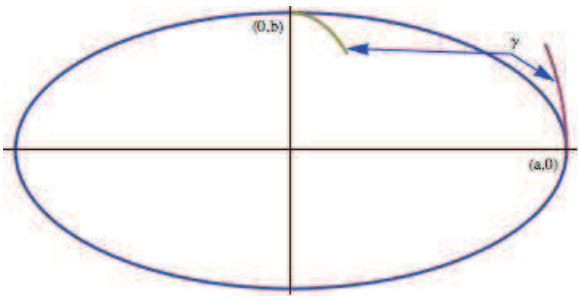

FIGURE 9. The Ellipse Serves as a Barrier for γ

However, an arrangement such as the one indicated in Figure 9 is impossible as it violates the monotone nature of *both* k and h. Therefore, it is impossible for $P(a) = \pi$, and since $P(c_1) = P(1) = 2\pi/\sqrt{2} > \pi$, the continuity of $P(a)$ ensures that $P(a) > \pi$. □

Corrolary 2.1. *The only embedded geodesics in $\mathcal{G}^2$ are lines through the origin and the unit circle.*

Proof. We already know that if γ parameterizes a straight line through the origin or the unit circle, then γ is a Gaussian-weighted geodesic. We need only address the cases when γ is strictly convex with $a \in (1, \infty)$. The period for such an embedded curve would be of the form $P = 2\pi/n$. However, we have already established that for strictly convex geodesics, $\pi < P < 2\pi$. These inequalities disallow *any* choice of n. Therefore, there are no other embedded geodesics, save the unit circle and lines through the origin. □

Remark 2.2. *In* [1] *the period function $P(a)$ is proven to be monotone decreasing in on $[1, \infty)$; this is illustrated in Figure 10.*

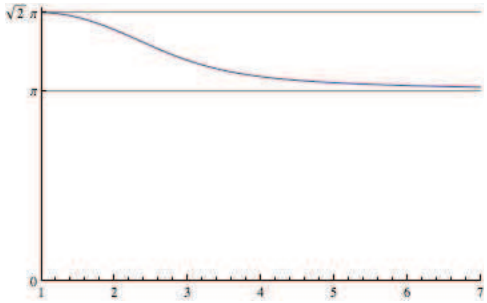

FIGURE 10. Plot of $P(a) = P(a, 0)$

As a result, one can uniquely classify all *of the closed geodesics in $\mathcal{G}^2$ as follows: A geodesic in $\mathcal{G}^2$ is closed if and only if the ratio of its winding number, m, to its petal-number, n, satisfies*

$$\frac{1}{2} < \frac{m}{n} < \frac{1}{\sqrt{2}}.$$

Other methods, such as those developed in [5]*, can also be deployed and adjusted to determine the monotonicity of $P(a)$. However, these arguments do not fit the tone and scope of this article, nor are they necessary for our results.*

Moreover, such methods are difficult to extend to the period functions $P(a, c)$ when $c \neq 0$. As noted in the previous section, when $c \neq 0$, the monotonicity of $P(a, c)$ is questionable. Our own numerical evidence and graphical plots demonstrate the existence of non-monotonic period functions, but the relationship between c and the behavior of $P(a, c)$ remains an interesting, open area of research.

2.3. **Self Shrinkers and Mean Curvature Flow.** As it turns out, equation (5) has been studied for decades and under remarkably different pretenses. Gaussian-weighted geodesics were first used by Physicist W.W. Mullins to model the motion of idealized grain boundaries (see [15]) but

are perhaps best known for homothetically shrinking under mean curvature flow. This flow is generated by

$$\frac{\partial \gamma}{\partial t} = -\kappa\, \vec{n} \tag{20}$$

where the normal $\vec{n}$ is outward pointing, $\kappa = |k|$ is the unsigned curvature, and t is a "time" parameter. If γ shrinks or expands under this flow, then $\gamma(s,t) = g(t)\gamma(s)$ and equation (20) becomes

$$g'(t)\gamma(s) = -\frac{\kappa(s)}{g(t)}\vec{n}(s).$$

Naturally, one sets $g(0) = 1$, and has $g'(0) < 0$ for shrinking curves while $g'(0) > 0$ for expanding ones. After separating variables and taking an inner product with the outward normal $\vec{n}$, one recovers our equation

$$h = \pm\kappa.$$

Note that a choice of a positive sign corresponds to a shrinker while a negative sign produces an expander. Shrinking curves were studied by Abresch and Langer in [1], leading to their classification mentioned in Remark 2.2, and curves featuring other kinds of self-similiarty have recently been studied by Halldorsson in [12].

3. Periodic Hypersurfaces in $\mathcal{G}^m$ with Constant Curvature

Minimal hypersurfaces in $\mathcal{G}^m$ as well as ones subjected to other, general densities have been studied, for instance, in [14] and [13]. Any hyperplane through the origin qualifies as a minimal surface in $\mathcal{G}^m$, for instance, since both $h = \langle \vec{x}, n\rangle$ and H vanish. Indeed, any general-position hyperplane in $\mathcal{G}^m$ has constant weighted mean curvature.

Hypersurfaces in $\mathcal{G}^m$ with constant weighted mean curvature that are also invariant under rigid motions are less numerous than classical CMC surfaces with analogous properties. This is more precisely evidenced by the following

Theorem 3.1. *Let $m \geq 3$ and suppose $S \subset \mathcal{G}^m$ is a hypersurface with constant weighted mean curvature. If S is periodic then S is of the form*

$$S = S' \times \mathbb{R}$$

where $S' \subset \mathcal{G}^{m-1}$ is a hypersurface with constant weighted-mean curvature.

Proof. Suppose $S \subset \mathbb{R}^m$ satisfies $H_\varphi = H + \frac{1}{m-1}h = c$ and is invariant under the set of translations $T_i(\vec{x}) = \vec{x} + \vec{v}_i$ where the vectors $\vec{v}_i$ span a non-trivial subspace and $1 \leq i \leq m$. (When $m = 3$, we call S "triply periodic, doubly periodic," or "singly periodic" in accordance with the dimension of this subspace.)

Without loss of generality, suppose $\vec{v}_m \neq \vec{0}$ and that $\vec{v}_m = z_0\vec{e}_m$. Since the mean curvature, H, is invariant under the translation $\vec{x} \mapsto \vec{x} + z_0\vec{e}_m$, it follows that the support function is also invariant under this translation. This means that for all $\vec{x} \in S$

$$\begin{aligned} & h(\vec{x}) = h(\vec{x} + z_0\vec{e}_m) \\ \iff & \langle \vec{x}, n\rangle = \langle \vec{x} + z_0\vec{e}_m, n\rangle = \langle \vec{x}, n\rangle + z_0\langle \vec{e}_m, n\rangle \\ \iff & 0 = z_0\langle \vec{e}_m, n\rangle \end{aligned}$$

which itself implies that the outward unit normal n is always perpendicular to $\vec{e}_m$. Hence, our surface S is of the form

$$S = S' \times \mathbb{R}.$$

It also follows that the support function for S evaluated at $\vec{x} = (x_1, \ldots, x_m) \in S$ agrees with the support function for S' evaluated at the projected point $\vec{x}' = (x_1, \ldots, x_{m-1}) \in S'$ – we will let h denote the support functions for both surfaces. Additionally, the mean curvature for S and S' are related via the equation

$$H = \frac{m-2}{m-1}H'$$

and since

$$H + \frac{1}{m-1}h = c$$

it also follows that

$$\left(\frac{m-2}{m-1}\right)H' + \frac{1}{m-1}h = c$$

$$\Rightarrow H' + \frac{1}{m-2}h = c\left(\frac{m-1}{m-2}\right)$$

which implies that the surface S' has constant weighted mean curvature, too. □

Corrolary 3.1. *The only periodic hypersurfaces in $\mathcal{G}^3$ with constant weighted mean curvature $H_\varphi = c$ are planes and rotated cylinders $\gamma \times \mathbb{R}$ where γ satisfies $h + k = 2c$.*

Proof. This follows immediately from Theorem 3.1. We are free to rotate the vertical cylinders $\gamma \times \mathbb{R}$ about the origin since our density function is, itself, symmetric about the origin. □

Corrolary 3.2. *The only embedded, periodic minimal surfaces in $\mathcal{G}^3$ are planes through the origin and circular cylinders of radius one whose axes are lines through the origin. In particular, there are no triply periodic minimal surfaces in $\mathcal{G}^3$.*

Proof. Again, this follows immediately from Theorem 3.1 with $c = 0$. Lines through the origin in $\mathcal{G}^2$ lift to planes through the origin in $\mathcal{G}^3$ and can then be rotated to produce *any* plane through the origin. The only other embedded geodesic in $\mathcal{G}^2$ is the unit circle, and after lifting it vertically, the resulting cylinder can similarly be rotated about the origin. □

Corollary 3.2 contrasts the rich theory of *classical*, periodic minimal surfaces in $\mathbb{R}^3$. Families of singly periodic, doubly periodic, and triply periodic minimal surfaces abound, including examples with interesting and rich topology (see [6], [9], [10], [16], and [17]).

Moreover, the techniques used in the proof of Theorem 3.1 apply equally well in proving that general cylinders, $S' \times I$, are also the only helicoidal surfaces with constant weighted mean curvature in $\mathcal{G}^3$. We say a surface $S \subset \mathbb{R}^3$ is *helicoidal* if it is invariant under a screw motion. An example of a vertical screw motion is given by the mapping

$$A(x, y, z) = (x \cos t - y \sin t, x \sin t + y \cos t, z + t\, z_0)$$

where $t, z_0 \in \mathbb{R}$ are fixed. Note that the action by A can be expressed in terms of a rotation matrix O and a vertical translation: $A\vec{x} = O\vec{x} + tz_0\vec{e}_3$ where O is a rotation of t-radians about the z-axis.

Theorem 3.2. *Suppose $S \subset \mathcal{G}^3$ has constant weighted mean curvature and is invariant under a screw motion. Then $S = \gamma \times I$ where γ is a curve in $\mathcal{G}^2 \times \{0\}$ with constant weighted curvature.*

Proof. Assume $S \subset \mathcal{G}^3$ has constant weighted mean curvature and is invariant under a screw motion. After a rotation, we may assume that the screw motion is vertical and so has the form given by A above. Since H is invariant under this motion and $H_\varphi = H - h/2 = c$, it follows that h is also invariant under A. In particular, if we let $\vec{y} = A\vec{x}$, then

$$\begin{aligned} h(\vec{x}) = \langle \vec{x}, n(\vec{x})\rangle = \langle \vec{y}, n(\vec{y})\rangle &= h(\vec{y}) \\ \Rightarrow \langle \vec{x}, n(\vec{x})\rangle = \langle O\vec{x} + t\, z_0\vec{e}_3, On(\vec{x})\rangle &= \langle O\vec{x}, On(\vec{x})\rangle + tz_0\langle \vec{e_3}, On(\vec{x})\rangle \\ \Rightarrow \langle \vec{x}, n\rangle = \langle \vec{x}, n\rangle &+ tz_0\langle O\vec{e}_3, On\rangle \\ \Rightarrow 0 = \langle O\vec{e}_3, On\rangle &= \langle \vec{e}_3, n\rangle \end{aligned}$$

and so n is horizontal, implying $S = \gamma \times I$. The same reasoning that was used at this point in the proof of Theorem 3.2 applies here, and so γ is itself a curve of constant weighted mean curvature. □

Corrolary 3.3. *The only embedded minimal helicoidal surface in $\mathcal{G}^3$ is a unit-radius cylinder centered about a line through the origin.*

Proof. This follows immediately from Theorem 3.2 and Corollary 2.1. □

References

[1] U. Abresch and J. Langer. The normalized curve shortening flow and homothetic solutions. *J. of Differential Geom.*, 23(2):109–205, 1986.

[2] E. Adams, I. Corwin, D. Davis, M. Lee, and R. Visocchi. Isoperimetric regions in gauss sectors. *Rose-Hulman Und. Math. J.*, 8(1), 2007.

[3] L. Ahlfors. *Conformal Invariants: topics in geometric function theory.* McGraw-Hill Series in Higher Mathematics. McGraw-Hill Book Co., New York-Düsseldorf-Johannesburg, 1973.

[4] C. Carroll, A. Jacob, C. Quinn, and R. Walters. The isoperimetric problem on planes with density. *Bulletin of the Australian Mathematical Society*, 78(02):177–197, October 2008.

[5] C. Chicone. The monotonicity of the period function for planar Hamiltonian vector fields. *J. Differential Equations*, 69(3):310–321, 1987.

[6] P. Connor and M. Weber. The construction of doubly periodic minimal surfaces via balance equations. *Amer. J. Math.*, 134(5):1275–1301, 2012.

[7] I. Corwin, N. Hoffman, S. Hurder, V. Sesum, and Y. Xu. Differential geometry of manifolds with density. *Rose-Hulman Und. Math J.*, 7(1), 2006.

[8] D DeTurck, H Gluck, D Pomerleano, and D S Vick. The four vertex theorem and its converse. *Notices Amer. Math. Soc.*, 54(2):192–207, 2007.
[9] C. Douglas. Genus one Scherk surfaces and their limits. *J. Differential Geom.*, 96(1):1–59, 2014.
[10] S. Fujimori and M. Weber. Triply periodic minimal surfaces bounded by vertical symmetry planes. *Manuscripta Math.*, 129(1):29–53, 2009.
[11] M. Gromov. Isoperimetry of waists and concentration of maps. *Geom. Func. Anal.*, 13:178–215, 2003.
[12] H. P. Halldorsson. Self-similar solutions to the curve shortening flow. *Trans. Amer. Math. Soc.*, 364(10):5285–5309, 2012.
[13] Doan The Hieu and N. M. Hoang. Ruled minimal surfaces in $\mathbb{R}^3$ with density e^z. *Pacific J. Math.*, 243(2):277–285, 2009.
[14] F. Morgan. Manifolds with density. *Notices Amer. Math. Soc.*, 52(8):853–858, 2005.
[15] W. W. Mullins. Two-dimensional motion of idealized grain boundaries. *J. Appl. Phys.*, 27:900–904, 1956.
[16] M. Weber. The genus-one helicoid as a limit of screw-motion invariant helicoids with handles. In *Global theory of minimal surfaces*, volume 2, pages 243–258. Amer. Math. Soc., Providence, RI, 2005.
[17] A. Weyhaupt. Deformations of the gyroid and Lidinoid minimal surfaces. *Pacific J. Math.*, 235(1):137–171, 2008.

DEPARTMENT OF MATHEMATICS AND COMPUTER SCIENCE
ST. MARY'S COLLEGE OF MARYLAND
ST. MARY'S CITY, MD, 20686
E-mail address: cjdouglas@smcm.edu